Biochimica et Biophysica Acta 1798 (2010) 338–343

Contents lists available at ScienceDirect

Biochimica et Biophysica Acta

journal homepage: www.elsevier.com/locate/bbamem

Assessing the uptake kinetics and internalization mechanisms of cell-penetrating peptides using a quenched fluorescence assay

Imre Mäger [a,b,*], Emelía Eiríksdóttir [b], Kent Langel [a], Samir EL Andaloussi [a,b], Ülo Langel [a,b]

[a] University of Tartu, Institute of Technology, Nooruse 1-517, 50411 Tartu, Estonia
[b] Stockholm University, Department of Neurochemistry, Stockholm, Sweden

ARTICLE INFO

Article history:
Received 6 May 2009
Received in revised form 25 September 2009
Accepted 2 November 2009
Available online 10 November 2009

Keywords:
Cell-penetrating peptide
Uptake kinetic
Uptake mechanism
Endocytosis inhibitor

ABSTRACT

Cell-penetrating peptides (CPPs) have shown great potency for cargo delivery both *in vitro* and *in vivo*. Different biologically relevant molecules need to be delivered into appropriate cellular compartments in order to be active, for instance certain drugs/molecules, e.g. antisense oligonucleotides, peptides, and cytotoxic agents require delivery into the cytoplasm. Assessing uptake mechanisms of CPPs can help to develop novel and more potent cellular delivery vectors, especially in cases when reaching a specific intracellular target requires involvement of a specific internalization pathway. Here we measure the overall uptake kinetics, with emphasis on cytoplasmic delivery, of three cell-penetrating peptides M918, TP10 and *p*Vec using a quenched fluorescence assay. We show that both the uptake levels and kinetic constants depend on the endocytosis inhibitors used in the experiments. In addition, in some cases only the internalization rate is affected by the endocytosis inhibitors while the total uptake level is not and vice versa, which emphasizes importance of kinetic studies when assessing the uptake mechanisms of CPPs. Also, there seems to be a correlation between lower total cellular uptake and higher first-order rate constants. Furthermore, this may indicate simultaneous involvement of different endocytic pathways with different efficacies in the internalization process, as hypothesized but not shown earlier in an uptake kinetics assay.

1. Introduction

Cell-penetrating peptides are short cationic and/or amphipathic peptides that are able to transport various molecules into mammalian cells. After the discovery of the first CPPs, Anntennapedia-derived peptide, now known as penetratin [1] and Tat peptide [2] the research in this field has been highly active since CPPs have shown great potency in cargo delivery both *in vitro* and *in vivo* [3–7].

Many novel CPPs have been developed in search for more effective transport vectors and there are even attempts made to predict cell-penetrating sequences [8]. Several CPP targeting schemes have been developed in order to turn these vectors into cell-specific cargo carriers [9–11].

Over the years several internalization mechanisms have been proposed to be involved in CPP uptake, ranging from direct translocation, transient pore formation and inverted micelle models to various subtypes of endocytosis, as shortly reviewed in [3]. Whereas non-endocytic translocation of CPPs without cargo molecules has been reported [12,13] the consensus among researchers appears to be that various types of endocytosis are exploited in the uptake of larger CPP-cargo constructs, and that several cell-entry mechanisms might act in parallel [14–17]. Also, it has been shown that the uptake can depend on whether the CPP is labeled or not, the type of cargo molecule used, and where the cargo is positioned in the CPP [18]. Further, it is important to take into consideration how the uptake is registered–whether a biological effect (e.g. splice correction) or just intracellular fluorescence of the labeled CPPs is measured–especially when the delivery of therapeutic molecules is under investigation since high total uptake level is not necessarily correlating with the biological effect of the cargo [19].

Several drugs and bioactive molecules need to reach the cytosol in order to mediate their biological effect [20–21]. Therefore, it is essential to evaluate which CPPs would be the best candidates for cytoplasmic delivery in terms of total uptake. Also, assessing the uptake mechanisms is of great importance since knowing the mechanisms facilitates the development of novel and more potent CPPs. Simple end-point uptake measurements in presence of endocytosis inhibitors may not reflect the inhibition effects precisely because if a certain inhibitor only affects the rate of uptake, the inhibition effect will depend largely on the chosen end-point. By registering also the uptake kinetics some more light might be shed on the possible internalization mechanisms of CPPs since one more parameter–the first-order rate constant of the uptake–will be revealed in these experiments. To our knowledge no attempts have been made so far to quantify the effect of endocytosis inhibitors on real time uptake kinetics.

* Corresponding author. University of Tartu, Institute of Technology, Nooruse 1-517, 50411 Tartu, Estonia. Fax: +372 7374900
E-mail address: imre.mager@ut.ee (I. Mäger).

0005-2736/$ – see front matter © 2009 Elsevier B.V. All rights reserved.
doi:10.1016/j.bbamem.2009.11.001

To address these issues we have measured the overall cargo delivery kinetics, with emphasis on cytoplasmic delivery, of three established CPPs M918, TP10 and *p*Vec. We measured the uptake kinetics using a quenched fluorescence assay [22] with some modifications. The results show that the uptake levels and rate constants depend on the endocytosis inhibitors used in the experiments and that, surprisingly, lower uptake levels often correlate with higher first-order rate constants. This may indicate simultaneous involvement of different endocytic pathways in the uptake of CPPs.

2. Experimental procedures

2.1. Peptide synthesis

Cargo peptide, TP10, and *p*Vec were synthesized stepwise on ABI 433A peptide synthesizer on 4-methylbenzhydrylamine (MBHA) resin using *t*-Boc chemistry. Amino acids were coupled as HOBt (hydroxybenzotriazole) esters using DCC (*N,N*'-dicyclohexylcarbodiimide) and DIEA (*N,N*'-Diisopropylethylamine). The M918 peptide was synthesized stepwise on ABI 433A (Applied Biosystems) synthesizer on rink amide MBHA resin using Fmoc chemistry. Amino acids were coupled as HOBt (hydroxybenzotriazole) esters using TBTU (2-(1H-Benzotriazole-1-yl)-1,1,3,3-tetramethylaminium tetrafluoroborate) and DIEA (*N,N*'-Diisopropylethylamine). In order to facilitate disulfide coupling, additional Cys(NPys) was manually coupled to the cargo peptide and a Cys residue was coupled to the N-termini of M918 and *p*Vec, and to the ε-amino group on Lys^7 of TP10. The cargo peptide was thereafter manually labeled N-terminally with a fluorescent molecule Abz (2-amino benzoic acid) and His(DNP) was coupled manually to the last cysteine of the CPPs to allow the DNP (dinitrophenol) moiety to act as a quencher for the Abz group. For peptide sequences see Table 1. After cleaving the peptides from the solid support, final products were purified with a reverse phase HPLC Supelco C18 column by using Dionex HPLC system, and the correct molecular masses were verified using Perkin-Elmer prOTOF 2000 MALDI O-TOF mass spectrometer.

2.2. Conjugation of the cargo peptide and CPPs

Abz-C(NPys)-Cargo peptide and His(DNP)-C-CPPs were conjugated via a disulfide bond. The reaction was carried out in DMF (*N,N*-dimethylformamide) supplemented with 10% DMSO (dimethyl sulfoxide) for 4 h. Thereafter, cargo-SS-CPP conjugates were purified with a reverse phase HPLC Supelco C18 column by using Dionex HPLC system, and the correct molecular mass verified using Perkin-Elmer prOTOF 2000 MALDI O-TOF mass spectrometer.

2.3. Cell culture

HeLa cells were grown in DMEM (Dulbecco's modified Eagle's medium) with glutamax, supplemented with 0.1 mM non-essential amino acids, 1.0 mM sodium pyruvate, 10% FBS (fetal bovine serum), 100 U/ml penicillin, and 100 mg/ml streptomycin. Cells were grown in 5.0% CO_2 atmosphere at 37 °C.

Table 1
Peptide sequences.

Name	Sequence
Cargo	Abz-C(NPys)-LKANL-amide
TP10	AGYLLGKINLKALAALAKKIL-amide[a]
*p*Vec	LLIILRRRIRKQAHAHSK-amide[a]
M918	MVTVLFRRLRIRRASGPPRVRV-amide[a]

[a] Underlined amino acids mark position where His(DNP)-Cys moiety is coupled to. For structures see Fig. 1A.

2.4. Endocytosis inhibitors

In order to assess internalization mechanisms of the cargo-SS-CPP constructs, the following endocytosis inhibitors were used: 10 μM chlorpromazine, 4 μM cytochalasin D, 50 nM wortmannin, 0.4 M sucrose. Cytochalasin D was used to block actin polymerization and hence the formation of macropinosomes [23], and wortmannin was used to inhibit clathrin mediated endocytosis by inhibiting PI3-kinase [23]. Both chlorpromazine [24] and sucrose [25] were utilized in order to inhibit clathrin mediated endocytosis. Chloroquine, a widely used endosomolytic agent, was left out of this study due to high interference with the fluorescent readout.

2.5. Uptake kinetics experiments

Two days prior to experiment HeLa cells were seeded onto a 10-cm cell culture dish to reach 90% confluency on the day of the experiment. Before treatment with peptides, cells were washed with PBS (phosphate buffered saline) and detached from the culture dish by incubating in 1 ml solution of 3 mM EDTA (ethylenediaminetetraacetic acid). Then 4 ml of DMEM supplemented with 10% FBS was added after which the cells were counted. Cells were centrifuged at $500 \times g$ for 10 min, supernatant was removed and the cells were resuspended in HKR (HEPES-buffered Krebs–Ringer solution) supplemented with 1 mg/ml glucose (HKRg) to have approximately 2.5×10^6 cells/ml (1.25×10^5 cells in 50 μl).

Kinetic measurements were performed in white 96-well plates according to the following protocol. 150 μl of the cargo-SS-CPP conjugates, prepared and diluted in HKRg, were added to the wells of the 96-well plate, while the plate was kept on ice. After 30 min approximately 125,000 cells in 50 μl were added to each well, to reach the final incubation volume of 200 μl and the final concentration of the cargo-SS-CPP conjugates of 1, 2.5 or 5 μM. Experiments in the presence of endocytosis inhibitors were carried out in a similar way; but first the suspended cells were pre-incubated for 30 min at 37 °C with corresponding endocytosis inhibitor after which the cells were added to each well that contained the conjugate solution with corresponding endocytosis inhibitor.

Thereafter, the plate was transferred to SPECTRAmax GEMINI XS (Molecular Devices, USA) fluorometer and the fluorescence was measured (excitation wavelength 320 nm, emission wavelength 420 nm). All the measurements were carried out at 37 °C in atmospheric CO_2 concentration. Data points were recorded in 35 s time interval, between each measurement the plate was shaken for 5 s to keep the cells in suspension. After 80 min the cells were lysed and TCEP (tris(2-carboxyethyl)phosphine) was added to each well to reach the final concentration of 100 μM to reduce all remaining disulfide bonds. The resulting signal described the fluorescence level which arises if the disulfide bonds between each cargo-SS-CPP molecule are cleaved at a given concentration. These data were used to normalize measured fluorescence values and to present the uptake data in picomoles of delivered constructs.

In order to verify weather the cargo peptide was membrane impermeable or not in our system, a cargo peptide carrying the quencher molecule instead of the fluorophore was synthesized. This molecule was conjugated to the original cargo peptide and the cells were incubated with 5 μM of that construct. The same construct served also as a negative control of the uptake.

We additionally verified that the observed cytoplasmic delivery of the CPP-cargo constructs is not an artifact form the disulfide reduction on the cell membrane or in the extracellular environment due to possible glutathione outflow from the cells. For these control experiments the cells were prepared as described above and treated with 5 μM cargo-SS-CPP conjugates in 1.5 ml Eppendorf tubes. At different time points (0, 30, 60 and 90 min) the cells were spun down, 100 μl of supernatant was removed and mixed with 50 μl of 6 mM

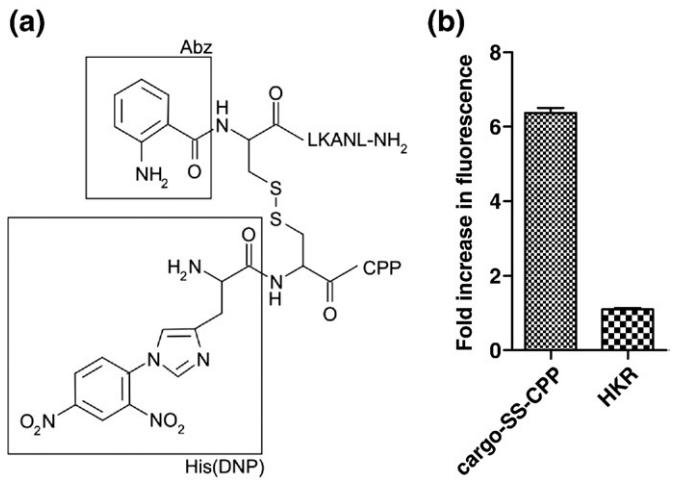

Fig. 1. (A) Structure of cargo-SS-CPP construct in quenched fluorescence assay. (B) A representative sample of a cargo-SS-CPP construct in quenched fluorescence assay. The fluorescence of a 10 μM sample in HKRg (HEPES-buffered Krebs–Ringer solution, supplemented with 1 mg/ml glucose) is measured before and after reducing the disulfide bonds with TCEP. When the construct is not present then fluorescence of the buffer does not increase. The error bars indicate S.E.M., number of samples is 3.

Ellman's reagent (5, 5′-dithiobis-(2-nitrobenzoic acid) or DTNB). Ellman's reagent reacts with free thiols, releasing 2-nitro-5-thiobenzoate (TNB^-), which ionizes to yellow TNB^{2-}. By monitoring absorption at 405 nm at various time points it can be demonstrated weather the free thiol concentration in the extracellular media is increasing or not. The absorption was measured in triplicates on a 96-well plate using a Tecan Sunrise microplate absorbance reader (Tecan Group Ltd., Switzerland). The data were normalized to the absorbance of the DTNB treated supernatant of lysed cells.

3. Results

Measurement of Abz-Cys-LKANL-amide pentapeptide uptake kinetics mediated by selected CPPs was described by Hällbrink et al. [22]. This assay is based on measurement of the increase in fluorescence using an energy transfer quenching method where the Abz molecule acts as a fluorophore and nitrotyrosine acts as a quencher [22]. However, in that work the CPP-mediated uptake mechanisms were not elucidated and the uptake kinetics was measured on different set of CPPs.

In the current work the quencher is changed. The side chain protective group of His, DNP, was used as a quencher in order to increase synthesis yields (Fig. 1A). In principle, when Abz-labeled cargo and CPP are conjugated via a disulfide linker, the Abz and DNP molecules are in close proximity, and the fluorescence of the Abz molecule (excitation: 320 nm, emission: 420 nm) is quenched by the DNP component. Once the disulfide bridge is cleaved, the fluorophore and quencher will drift apart and increase of fluorescence signal is registered. This is shown in Fig. 1B where 10 μM cargo-SS-CPP construct in HKRg is treated with 100 μM TCEP. The data is represented as fold increase in fluorescence signal before and after TCEP treatment. Intracellularly the disulfide bond is reduced by glutathione and increase in fluorescence signal reflects the overall uptake arising from released cargo molecules.

We evaluated three different CPPs (M918, TP10 and *p*Vec) for their ability to deliver pentapeptide cargo into HeLa cells with and without the presence of endocytosis inhibitors. Uptake kinetic curves were registered and the measured data points were fitted to one-phase exponential association curves with GraphPad Prism software (GraphPad Software, Inc., USA), according to the formula

$$Y = Y_{max} \cdot [1 - \exp(-K \cdot x)] \quad \text{(Eq.1)}$$

where Y is the uptake level (picomoles of internalized peptide), Y_{max} is the maximal uptake level, K is the first-order rate constant in s^{-1}, and x is time in s. The first-order rate constants were determined from the fitted curves, as well as exponential association plateau values.

3.1. The uptake kinetics is dependent on peptide concentration

Before measuring uptake kinetics of cargo-SS-CPP constructs we verified weather the cargo peptide was membrane impermeable or not in our system. For this purpose we synthesized also a cargo peptide carrying the quencher molecule instead of the fluorophore. We conjugated these two different types of cargo molecules and incubated the cells with 5 μM of that construct. We did not observe any increase of fluorescence during 60 min incubation (data not shown).

Not surprisingly, the peptide uptake curves depend on the peptide concentration. The results of different experiments carried out on different days are repeatable. The K values determined from the experiments conducted on different days vary in range of 5%, but the difference in plateau values is somewhat greater, reaching 10% (data not shown), most probably depending on the actual number of suspended cells added to the peptide solutions in the 96-well plate. The results of the uptake experiments, performed in triplicates, at three different conjugate concentrations (1, 2.5 and 5 μM) with the

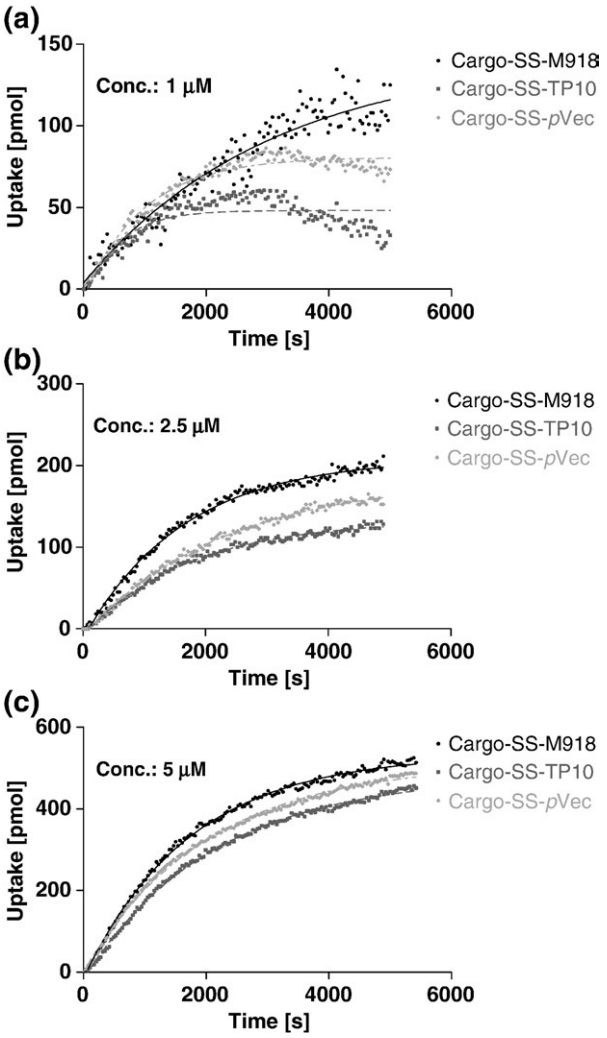

Fig. 2. Cargo-SS-CPP uptake curves, for concentrations 1 μM (A), 2.5 μM (B) and 5 μM (C). The curves are plotted as mean values of triplicate experiment and non-linear regression curves according to Eq. (1).

Table 2
Uptake rate constants and plateau values.

Cargo-SS-CPP	Cargo-SS-CPP concentration		
	1 μM	2.5 μM	5 μM
	Rate constants ($K \pm SD$) $\times 10^{-4}$ s^{-1}		
Cargo-SS-M918	2.00 ± 0.65 (3)	6.08 ± 0.35 (3)	5.74 ± 0.11 (3)
Cargo-SS-TP10	13.92 ± 0.79 (3)	5.73 ± 0.15 (3)	4.71 ± 0.15 (3)
Cargo-SS-*p*Vec	8.48 ± 0.37 (3)	4.31 ± 0.10 (3)	4.98 ± 0.20 (3)
	Plateau values ($Y_{max} \pm SD$) pmol		
Cargo-SS-M918	143.1 ± 8.9 (3)	209.1 ± 4.0 (3)	534.3 ± 3.2 (3)
Cargo-SS-TP10	48.2 ± 0.8 (3)	133.8 ± 1.2 (3)	483.0 ± 5.7 (3)
Cargo-SS-*p*Vec	80.8 ± 0.8 (3)	184.1 ± 1.8 (3)	512.2 ± 6.8 (3)

three different CPPs (M918, TP10 and *p*Vec) are presented in Fig. 2 and Table 2.

Plateau values of the kinetic curves depend on concentration of the conjugates (Table 2), but a general relationship can be brought out; at each tested concentration M918 is superior to the other two, leaving TP10 with the lowest uptake level, in context of maximal uptake. It is notable that similar relationship does not apply for kinetic constants since kinetic constants vary to a greater extent in relation with concentration of the conjugates. We also observed that the free thiol content in the extracellular media is not changing during 90 min incubation with 5 μM cargo-SS-CPP constructs (Fig. 3).

3.2. Effect of endocytosis inhibitors on the uptake kinetics

Further on, the effect of the endocytosis inhibitors on the uptake curves was investigated. We chose a cargo-SS-CPP concentration of 2.5 μM. This concentration of CPPs that we used in the study, relying on the literature, is not toxic to the cells [18,26,27]. This is also confirmed by an LDH leakage assay which did not show higher toxicity levels of peptide-treated cells compared to untreated cells (data not shown). Cargo-SS-CPP concentration of 2.5 μM still retained high enough fluorescent signals to be measured by the fluorometer. Lowering the construct's concentration even more led to low signal-to-noise ratio and these concentrations were left out of this study. The inhibitors used in these experiments were 10 μM chlorpromazine, 4 μM cytochalasin D, 50 nM wortmannin, and 0.4 M sucrose; the concentrations were chosen based on previous experience in our lab [19,28,29]. The results of these experiments are presented in Fig. 4.

Endocytosis inhibitors affect both the first-order rate constant and the total uptake level of cargo-SS-CPP constructs, although the inhibition effects vary between CPPs. For instance, the endocytosis inhibitors have the strongest effect on M918-mediated uptake, whereas *p*Vec-mediated uptake is less affected by the inhibitors.

Judging from Fig. 4 there seems to be several different pathways involved in the uptake of the conjugates that are affected by different

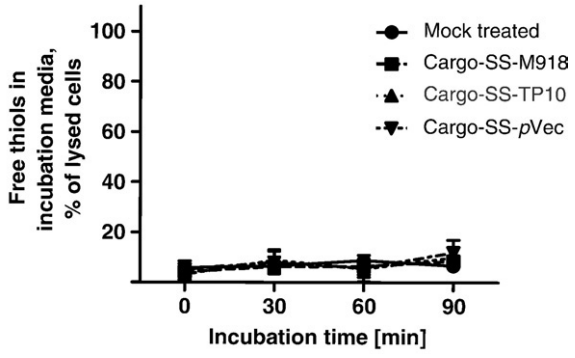

Fig. 3. Free thiol content in the incubation media is not changed when the cells are incubated in 5 μM cargo-SS-CPP constructs or simply in HKRg (mock-treated sample). The experiments were carried out in triplicates. For experimental conditions, see Experimental procedures.

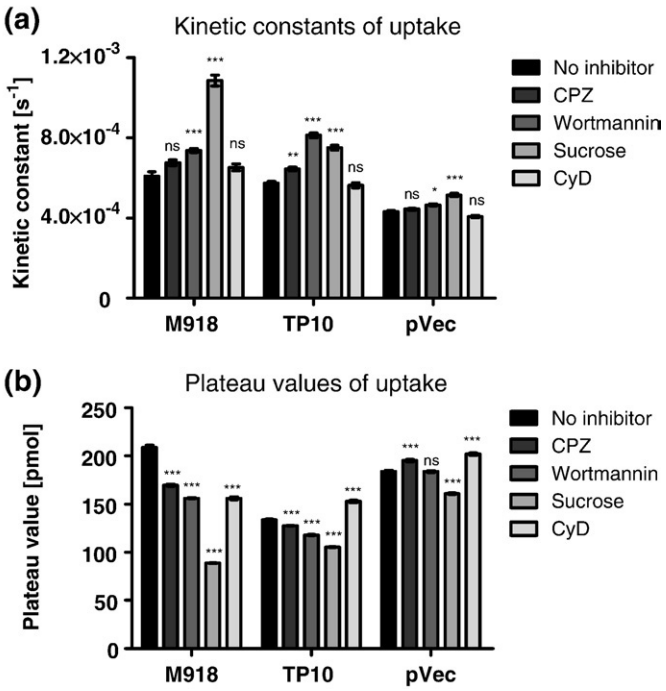

Fig. 4. First-order rate constants (A) and plateau values (B) of cargo-SS-CPP uptake in presence of different endocytosis inhibitors. Experiments were carried out with conjugate concentration of 2.5 μM. Mean values are compared with the control by one-way ANOVA analysis; *** marks significant difference $p<0.001$, ** marks significant difference $p<0.05$, and ns marks statistically non-significant difference. The error bars indicate S.E.M., number of samples is 3.

inhibitors to different extent. By using sucrose or wortmannin the first-order rate constant of M918 uptake increases, meaning that the plateau value of the uptake is reached in shorter time interval. At the same time the plateau values themselves in case of M918 and mentioned inhibitors are significantly lower compared to the control. Interestingly, cytochalasin D does not significantly change the kinetic constants but nevertheless reduce the plateau value of the uptake of M918.

For the TP10 conjugate, cytochalasin D is the only inhibitor that does not significantly affect the kinetic constant of the uptake while still increasing the plateau value. Wortmannin, chlorpromazine and sucrose increase the first-order rate constants of the uptake and decrease the total uptake levels.

For the *p*Vec conjugate it is observable that only cytochalasin D has statistically significant effect on both the kinetic constant and plateau value; the other inhibitors only affect the plateau values but not kinetic constants, except wortmannin that is ineffective for both parameters.

It is interesting that a general pattern between the kinetic constant and plateau values seems to be emerging. When the corresponding inhibitor increases the first-order rate constant, the plateau value of the uptake is decreased at the same time and vice versa, which is somewhat surprising. On the other hand, when a kinetic constant does not change significantly upon treatment with a certain inhibitor the same conclusion cannot be made for the corresponding plateau value.

4. Discussion

So far only few studies have been conducted to quantitatively characterize real time uptake kinetics. Previously the uptake kinetics of ^{125}I-biotinyl-transportan in Bowes' melanoma cells [30], NBD-penetratin in K562 cells [31,32], [^{99m}Tc]Tat [33] and fluoresceinyl-Tat in Jurkat cells [34], and rhodamine-labeled Tat, polyarginine [35,36],

transportan and penetratin [36] have been measured. Also measurement of the uptake kinetics of modified fluorescein-labeled polyarginine [37], fluorescein-labeled programmed cell death inducing cyclic hexapeptide conjugated to an arginine rich CPP [38], and fluorescein or TAMRA labeled L- or D-isomer, respectively, of polyarginine [13] has been recently reported. However, several different methods ranging from flow cytometry studies and spectrophotometry to mere microscopy observations have been used in these studies, which means that in many cases precise rate constants have not been characterized. Our intension was to measure these parameters in different experimental conditions in order to draw conclusions on the mechanisms of CPP translocation.

Here we used a quenched fluorescence assay [22] with small modifications. We use CPPs that carry two additional amino acids, a cysteine to allow disulfide bridging, and a histidine with dinitrophenol (DNP) side protecting group which serves as a quencher for the fluorescent Abz molecule. Abz is in turn coupled to the cargo peptide which also carries an additional cysteine for disulfide bridging. The cargo peptide itself is cell impermeable [22]. The structure of the designed constructs is presented in Fig. 1A.

Once the disulfide bond is cleaved, the fluorophore (Abz) and quencher (DNP) will drift apart. The quenching will be lost and increase in fluorescence is measured. It is a generally accepted fact that disulfide bonds are readily reduced in the cytoplasm by glutathione. Although it has been proposed that the reduction can occur in small extent also on the cell membrane of some cells and in some vesicular compartments mediated by protein disulfide isomerase or gamma-interferon-inducible lysosomal thiol reductase [39], and that the reduction may depend even on the peptide sequence [40], nevertheless, it has been shown that the vast majority, if not all of the reduction takes place in the cytoplasm [41]. Therefore, we measure reduction rate of disulfide bonds of cargo-SS-CPP conjugates which correlates with cytoplasmic delivery of these compounds.

In support of the latter conclusion is the fact that we do not see any change in the amount of free thiols in extracellular media during incubation of cells with cargo-SS-CPP conjugates (Fig. 3). This indicates that the constructs remain intact. Furthermore, this is consistent with the assumption that in this model system disulfide bonds are not cleaved on the cell membrane in a significant amount and reduction due to possible glutathione outflow from the cells is negligible. Furthermore, if conjugating fluorophore-labeled cargo peptide with the quencher-labeled cargo peptide we do not observe uptake either (data not shown). Apart from confirming that our cargo peptide is indeed membrane impermeable, this further demonstrates that the disulfide bond remains stable in the extracellular media.

Uptake kinetics of other CPPs by principally the same assay has been assessed before [22] but without using endocytosis inhibitors. In this study we evaluated effects of these inhibitors on the uptake kinetics in order to provide information on the uptake mechanism of the cargo-SS-CPP conjugates. The first-order rate constants we measured are in overall range of $0.2–1.4\times10^{-3}$ s^{-1}, with corresponding $t_{1/2}$ values in range of about 15–30 min. The range of measured rate constants is consistent with some of the previously published results in the field of CPPs where the $t_{1/2}$ values were found to be approximately 7, 12, 34 and 58 min for MAP, transportan, Tat and penetratin, respectively [22]; or 20 min [31] and 45 min [32] for NBD-labeled penetratin. On the other hand, for some peptides, the $t_{1/2}$ values of uptake have been shown to be even less than 2 min [33,35]. These differences might be a result of different cell types used in these experiments, different measurement methods, different labeling techniques and/or different uptake mechanisms that are exploited by different CPPs. We also measured the amount of internalized peptide which is in range of 48–534 pmol, corresponding to 18–60% of the added peptide (see Table 1 and Fig. 4) and these results are consistent with previously published studies where the same parameter has been measured [22,31,32].

The effect of endocytosis inhibitors on the first-order rate constants and plateau values of the uptake is apparent, with some common pattern between those two parameters. When the kinetic constant is significantly higher compared to the control, the plateau value of the uptake is generally lower than the control, and vice versa. On the other hand, when either of these parameters does not significantly differ from the control, no prediction can be made on the other parameter. This is a somewhat surprising result since generally one would expect that lower total penetration is accompanied by also slower uptake. But in our case, the obtained results indicate involvement of several different uptake pathways (various endocytotic routes, including clathrin mediated endocytosis, macropinocytosis, etc.) of these peptides which give rise to different patterns of releasing the conjugates into the cytosol. This is also consistent with previously published results [14–17].

Interestingly, by co-incubating cells with certain inhibitor/CPP combinations (for example cytochalasin D and TP10; or chlorpromazine or cytochalasin D with *p*Vec), the overall uptake of the conjugates seems to increase rather than decrease as would be expected from the treatment with an inhibitor. This may further suggest that different competing pathways may be involved simultaneously in the CPP mediated uptake process but with different efficacies [15], and when one rate-limiting pathway is inhibited, other pathways may be exploited to a greater extent. This hypothesis should, however, be tested more thoroughly in future studies in order to shed light onto this interesting matter.

Fluoresceinyl-labeled *p*Vec-PNA conjugates have previously displayed remarkable uptake but almost no biological effect in the nucleus by a splice correction assay [19]. Also, uptake of fluoresceinyl-labeled *p*Vec has been shown to decrease by 25% upon wortmannin treatment in human Bowes melanoma cells [42] but no significant effect of the corresponding inhibitor on the kinetic constant nor the plateau level of the uptake was observed in our case. Interestingly, that paper also claims that the uptake of *p*Vec is not significantly affected when the uptake experiments are performed at +8 °C [42]. The differences compared with our results might depend on the readout used. The cargo must reach the nucleus in order to produce a biological effect in one case [19] while in the other case registered total uptake may also contain large portion of signal rising from endosomaly entrapped CPPs [42]. In our case the main contributor to the readout is originating from the conjugates that have entered the cell cytoplasm. Our results suggest involvement of both macropinocytosis and clathrin mediated endocytosis in the uptake of cargo-SS-*p*Vec, although the relative effects of corresponding inhibitors compared to control remains relatively small and other pathways (endocytic or direct translocation) cannot be excluded based on our data.

In case of TP10 we observe significant increase in uptake levels by treating cells with cytochalasin D, and decreased uptake after treatment with chlorpromazine or wortmannin. This suggests a predominant involvement of clathrin mediated endocytosis. Lundin and coworkers [19] reported a similar trend in the splice correction assay with the same peptide, conjugated to splice correcting PNA. In addition, we also observe that lower uptake levels correspond to higher kinetic constants in case of TP10. In other words, the lower plateau values will be reached in less time and it seems that the limiting factor in overall uptake is not the maximal rate of a certain pathway but the overall capability of this pathway to be involved in this particular active transport pathway.

The M918 peptide displays decreased uptake when the cells are co-incubated with chlorpromazine, wortmannin, sucrose and cytochalasin D, suggesting both clathrin mediated endocytosis and macropinocytosis being involved extensively in the cellular delivery of the cargo peptide. This is consistent with previously published finding that the main contributors to the uptake of this peptide when conjugated to PNA are macropinocytosis and with lesser extent also

clathrin mediated endocytosis [19]. In another study the involvement of clathrin mediated endocytosis was observed when the uptake of M918 was inhibited by sucrose [26]. We also observe lower uptake values when using inhibitors with corresponding higher kinetic constants, suggesting that indeed there is more than one pathway simultaneously involved in the delivery also of this peptide.

In conclusion, by monitoring overall cytoplasmic delivery of CPPs by a quenched fluorescence assay we show that different CPPs might exploit different competing endocytotic internalization pathways simultaneously. Not only uptake levels but also the overall kinetic profile of the uptake is changed when cells are treated with different endocytosis inhibitors. We also observe that lower uptake levels often correlate with higher first-order rate constants. This is an important observation since majority of CPP delivery studies are single time-point measurements which may not take these specialties into account when efficacies of different CPPs are elucidated. Our results also are in accordance with the observation that different entry pathways may be involved in the delivery of cargo molecules to different cellular compartments even when using the same CPP.

Acknowledgements

The work presented in this article was supported by Swedish Research Council (VR-NT); by Center for Biomembrane Research, Stockholm; by Knut and Alice Wallenberg's Foundation; by the EU trough the European Regional Development Fund through the Center of Excellence in Chemical Biology, Estonia; by the targeted financing SF0180027s08 from the Estonian Government; by the DoRa Program of The European Social Fund; and by Archimedes Foundation.

References

[1] D. Derossi, A.H. Joliot, G. Chassaing, A. Prochiantz, The third helix of the Antennapedia homeodomain translocates through biological membranes, J. Biol. Chem. 269 (1994) 10444–10450.
[2] E. Vivès, P. Brodin, B. Lebleu, A truncated HIV-1 Tat protein basic domain rapidly translocates through the plasma membrane and accumulates in the cell nucleus, J. Biol. Chem. 272 (1997) 16010–16017.
[3] P. Järver, K. Langel, S. El-Andaloussi, Ü. Langel, Applications of cell-penetrating peptides in regulation of gene expression, Biochem. Soc. Trans. 35 (2007) 770–774.
[4] V. Kersemans, K. Kersemans, B. Cornelissen, Cell penetrating peptides for *in vivo* molecular imaging applications, Curr. Pharm. Des. 14 (2008) 2415–2447.
[5] C. Foged, H.M. Nielsen, Cell-penetrating peptides for drug delivery across membrane barriers, Expert Opin. Drug Deliv. 5 (2008) 105–117.
[6] L. Chen, S.D. Harrison, Cell-penetrating peptides in drug development: enabling intracellular targets, Biochem. Soc. Trans. 35 (2007) 821–825.
[7] R. Abes, A.A. Arzumanov, H.M. Moulton, S. Abes, G.D. Ivanova, P.L. Iversen, M.J. Gait, B. Lebleu, Cell-penetrating-peptide-based delivery of oligonucleotides: an overview, Biochem. Soc. Trans. 35 (2007) 775–779.
[8] M. Hansen, K. Kilk, Ü. Langel, Predicting cell-penetrating peptides, Adv. Drug Deliv. Rev. 60 (2008) 572–579.
[9] M. Essler, E. Ruoslahti, Molecular specialization of breast vasculature: a breast-homing phage-displayed peptide binds to aminopeptidase P in breast vasculature, Proc. Natl. Acad. Sci. U. S. A. 99 (2002) 2252–2257.
[10] V.A. Sethuraman, Y.H. Bae, TAT peptide-based micelle system for potential active targeting of anti-cancer agents to acidic solid tumors, J. Control. Release 118 (2007) 216–224.
[11] T. Jiang, E.S. Olson, Q.T. Nguyen, M. Roy, P.A. Jennings, R.Y. Tsien, Tumor imaging by means of proteolytic activation of cell-penetrating peptides, Proc. Natl. Acad. Sci. U. S. A. 101 (2004) 17867–17872.
[12] S. Futaki, I. Nakase, A. Tadokoro, T. Takeuchi, A.T. Jones, Arginine-rich peptides and their internalization mechanisms, Biochem. Soc. Trans. 35 (2007) 784–787.
[13] G. Tünnemann, G. Ter-Avetisyan, R.M. Martin, M. Stöckl, A. Herrmann, M. Cardoso, Live-cell analysis of cell penetration ability and toxicity of oligo-arginines, J. Pept. Sci. 14 (2008) 469–476.
[14] S. El-Andaloussi, T. Holm, Ü. Langel, Cell-penetrating peptides: mechanisms and applications, Curr. Pharm. Des. 11 (2005) 3597–3611.
[15] G.M.K. Poon, J. Gariépy, Cell-surface proteoglycans as molecular portals for cationic peptide and polymer entry into cells, Biochem. Soc. Trans. 35 (2007) 788–793.
[16] C. Foerg, H.P. Merkle, On the biomedical promise of cell penetrating peptides: limits versus prospects, J. Pharm. Sci. 97 (2008) 144–162.
[17] F. Duchardt, M. Fotin-Mleczek, H. Schwarz, R. Fischer, R. Brock, A comprehensive model for the cellular uptake of cationic cell-penetrating peptides, Traffic 8 (7) (2007) 848–866.
[18] S. El-Andaloussi, P. Järver, H.J. Johansson, Ü. Langel, Cargo-dependent cytotoxicity and delivery efficacy of cell-penetrating peptides: a comparative study, Biochem. J. 407 (2007) 285–292.
[19] P. Lundin, H. Johansson, P. Guterstam, T. Holm, M. Hansen, Ü. Langel, S. El-Andaloussi, Distinct uptake routes of cell-penetrating peptide conjugates, Bioconjug. Chem. 19 (2008) 2535–2542.
[20] P. Lundberg, S. El-Andaloussi, T. Sütlü, H. Johansson, Ü. Langel, Delivery of short interfering RNA using endosomolytic cell-penetrating peptides, FASEB J. 21 (2007) 2664–2671.
[21] T. Takeuchi, M. Kosuge, A. Tadokoro, Y. Sugiura, M. Nishi, M. Kawata, N. Sakai, S. Matile, S. Futaki, Direct and rapid cytosolic delivery using cell-penetrating peptides mediated by pyrenebutyrate, ACS Chem. Biol. 1 (2006) 299–303.
[22] M. Hällbrink, A. Florén, A. Elmquist, M. Pooga, T. Bartfai, Ü. Langel, Cargo delivery kinetics of cell-penetrating peptides, Biochim. Biophys. Acta 1515 (2001) 101–109.
[23] I. Nakase, M. Niwa, T. Takeuchi, K. Sonomura, N. Kawabata, Y. Koike, M. Takehashi, S. Tanaka, K. Ueda, J.C. Simpson, A.T. Jones, Y. Sugiura, S. Futaki, Cellular uptake of arginine-rich peptides: roles for macropinocytosis and actin rearrangement, Mol. Ther. 10 (2004) 1011–1022.
[24] G.D. Ivanova, A. Arzumanov, R. Abes, H. Yin, M.J.A. Wood, B. Lebleu, M.J. Gait, Improved cell-penetrating peptide-PNA conjugates for splicing redirection in HeLa cells and exon skipping in mdx mouse muscle, Nucleic Acids Res. 36 (2008) 6418–6428.
[25] J.E. Heuser, R.G. Anderson, Hypertonic media inhibit receptor-mediated endocytosis by blocking clathrin-coated pit formation, J. Cell Biol. 108 (1989) 389–400.
[26] S. El-Andaloussi, H.J. Johansson, T. Holm, Ü. Langel, A novel cell-penetrating peptide, M918, for efficient delivery of proteins and peptide nucleic acids, Mol. Ther. 15 (2007) 1820–1826.
[27] K. Saar, M. Lindgren, M. Hansen, E. Eiríksdóttir, Y. Jiang, K. Rosenthal-Aizman, M. Sassian, Ü. Langel, Cell-penetrating peptides: a comparative membrane toxicity study, Anal. Biochem. 345 (2005) 55–65.
[28] P. Säälik, A. Elmquist, M. Hansen, K. Padari, K. Saar, K. Viht, Ü. Langel, M. Pooga, Protein cargo delivery properties of cell-penetrating peptides. A comparative study, Bioconjug. Chem. 15 (2004) 1246–1253.
[29] S. El-Andaloussi, P. Guterstam, Ü. Langel, Assessing the delivery efficacy and internalization route of cell-penetrating peptides, Nat. Protoc. 2 (2007) 2043–2047.
[30] M. Pooga, M. Hällbrink, M. Zorko, Ü. Langel, Cell penetration by transportan, FASEB J. 12 (1998) 67–77.
[31] G. Drin, M. Mazel, P. Clair, D. Mathieu, M. Kaczorek, J. Temsamani, Physico-chemical requirements for cellular uptake of pAntp peptide. Role of lipid-binding affinity, Eur. J. Biochem. 268 (2001) 1304–1314.
[32] G. Drin, S. Cottin, E. Blanc, A.R. Rees, J. Temsamani, Studies on the internalization mechanism of cationic cell-penetrating peptides, J. Biol. Chem. 278 (2003) 31192–31201.
[33] V. Polyakov, V. Sharma, J.L. Dahlheimer, C.M. Pica, G.D. Luker, D. Piwnica-Worms, Novel Tat-peptide chelates for direct transduction of technetium-99m and rhenium into human cells for imaging and radiotherapy, Bioconjug. Chem. 11 (2000) 762–771.
[34] J.P. Richard, K. Melikov, E. Vives, C. Ramos, B. Verbeure, M.J. Gait, L.V. Chernomordik, B. Lebleu, Cell-penetrating peptides. A reevaluation of the mechanism of cellular uptake, J. Biol. Chem. 278 (2003) 585–590.
[35] T. Suzuki, S. Futaki, M. Niwa, S. Tanaka, K. Ueda, Y. Sugiura, Possible existence of common internalization mechanisms among arginine-rich peptides, J. Biol. Chem. 277 (2002) 2437–2443.
[36] S.W. Jones, R. Christison, K. Bundell, C.J. Voyce, S.M.V. Brockbank, P. Newham, M.A. Lindsay, Characterisation of cell-penetrating peptide-mediated peptide delivery, Br. J. Pharmacol. 145 (2005) 1093–1102.
[37] X. Li, R. Higashikubo, J. Taylor, Use of multiple carboxylates to increase intracellular retention of fluorescent probes following release from cell penetrating fluorogenic conjugates, Bioconjug. Chem. 19 (2008) 50–56.
[38] Y. Sasaki, M. Minamizawa, A. Ambo, S. Sugawara, Y. Ogawa, K. Nitta, Cell-penetrating peptide-conjugated XIAP-inhibitory cyclic hexapeptides enter into Jurkat cells and inhibit cell proliferation, FEBS J. 275 (2008) 6011–6021.
[39] G. Saito, J.A. Swanson, K. Lee, Drug delivery strategy utilizing conjugation via reversible disulfide linkages: role and site of cellular reducing activities, Adv. Drug. Deliv. Rev. 55 (2003) 199–215.
[40] S. Aubry, F. Burlina, E. Dupont, D. Delaroche, A. Joliot, S. Lavielle, G. Chassaing, S. Sagan, Cell-surface thiols affect cell entry of disulfide-conjugated peptides, FASEB J. (2009), doi:10.1096/fj.08-127563.
[41] W.C. Shen, H.J. Ryser, L. LaManna, Disulfide spacer between methotrexate and poly(D-lysine). A probe for exploring the reductive process in endocytosis, J. Biol. Chem. 260 (1985) 10905–10908.
[42] A. Elmquist, M. Hansen, Ü. Langel, Structure–activity relationship study of the cell-penetrating peptide pVEC, Biochim. Biophys. Acta 1758 (2006) 721–729.